Behavior of Reinforced Zero Cement Concrete Slabs under Monotonic Load

Maher M. Hassoon[1], Musab Aied Qissab[2*]

Authors affiliations:
1) Department of Civil Engineering, Al-NahrainUniversity, Baghdad-Iraq.
st.maher.m@ced.nahrainuniv.edu.iq

2*) Department of Civil Engineering, Al-Nahrain University, Baghdad-Iraq.
musab.a.jindeel@nahrainuniv.edu.iq

Paper History:

Received: 21st Apr. 2024

Revised: 7th Jul. 2024

Accepted: 14th Jul. 2024

Abstract

Searching for an optimal alternative to normal cement concrete (NCC) is an urgent need nowadays in order to reduce carbon dioxide emissions, reduce energy, and reduce waste materials. Therefore, this research aims to examine zero cement concrete (ZCC) slabs under monotonic loads with several paramedic studies including slab thickness (60mm, 80mm, 100 mm), bar spacing (75mm, 150mm, and 225mm), and molarity concentration (6M, 8M, and 10M). The results showed the behavior of reinforced ZCC slabs is similar to or slightly lower than that of normal cement concrete. Increasing slab thickness from 60 mm to 80 mm and 100 mm enhanced the slab stiffness, increased the applied loads, and reduced the vertical mid-span deflection. Decreasing bar spacing by 33.33% and 66.67% relative to 225 mm reduced also the deflection. The energy absorption was increased due to increasing the slab thickness and bar spacing. When the load increased, the slabs eventually failed by a typically visible punching cone (punching shear).

Keywords: Zero Cement Concrete, Molarity, Carbon Emission, Cement Industry.

سلاك البلطات الخرسانية المسلحةالخالية من الاسمنت تحت الاحمال الرتيبة

ماهر محمود حسون ، مصعب عايد كصب

الخلاصة:

أصبح البحث عن البديل الأمثل للخرسانة الأسمنتية العادية حاجة ملحة في الوقت الحاضر من أجل تقليل انبعاثات ثاني أكسيد الكربون وتقليل الطاقة وتقليل النفايات. ولذلك، يهدف هذا البحث إلى فحص البلاطات الخرسانية الأسمنتية الخالية من الاسمنت تحت الأحمال الرتيبة مع العديد من المتغيرات بما في ذلك سمك البلاطة (٦٠ م، ٨٠ م، ١٠٠ م)، وتباعد القضبان (٧٥ م، ١٥٠ م، و ٢٢٥ م)، والتركيز المولارى (M٦، ٨ م، و ١٠ م). أظهرت النتائج أن سلوك بلاطات ZCC المسلحة مشابه أو أقل قليلاً من سلوك الخرسانة الأسمنتية العادية. تؤدي زيادة سماكة البلاطة من ٦٠ م إلى ٨٠ م و ١٠٠ م إلى تحسين صلابة البلاطة وزيادة الأحمال المسلطة وتقليل الهطول العمودي الوسطي. كما أدى تقليل تباعد القضبان بنسبة ٣٣,٣٣٪ و٦٦,٦٧٪ مقارنة بـ ٢٢٥ ملم إلى تقليل الهطول أيضًا. تم زيادة امتصاص الطاقة بسبب زيادة سماكة البلاطة وتباعد القضبان. عندما زاد الحمل، فشلت السقوف في النهاية عن طريق مخروط التثقيب المرئي النموذجي (قص التثقيب)..

1. Introduction

Applications of civil engineering have improved over time in response to the growth of the building sector. The majority of the concrete used in the building industry is made mostly of Portland cement, sometimes referred to as conventional cement, which serves as binding material. Three-quarters of the energy utilized worldwide that resulted in carbon emissions came from the building and construction sector [1]. It has been determined that about one ton of CO_2 emissions are directly caused by the production of one ton of cement [2]. As a result, many researchers have looked for substitute techniques to cut down on or completely do away with the need for cement in concrete. Reports state that in order to keep global warming temperatures from rising above 1.5 C, the UN is pushing for green or carbon-free concrete and building by 2050 [3]. One of the best ways to reduce carbon dioxide emissions and the climate change challenge is to switch from traditional binding materials to green or zero-carbon

NJES is an open access Journal with ISSN 2521-9154 and eISSN 2521-9162
This work is licensed under a Creative Commons Attribution-NonCommercial 4.0 International License

building materials. The term "zero carbon concrete" (ZCC) refers to a number of different types of concrete that contain no cement at all. It was determined that ZCC offers more early strength, higher flexural strength, similar or slightly lower compressive strength, lower heat of hydration, faster hydration rate, and superior durability in a sulfate environment when compared to ordinary concrete [4]–[6].

Unlike normal concrete (NC), ZCC production is affected by numerous factors apart from the aggregate (coarse and fine) properties, i.e. binder material type, alkaline activator, molarity concentration, ratio of alkaline solution to binder, curing regime, temperature, superplasticizer, resting time, mixture design, modulus ratio or molar ratio (SiO_2/Na_2O), Sodium Silicate to Sodium Hydroxide (SS/SH), and mixing procedure [7]. The main difference is shown in Fig. 1. It was discovered that the most widely used aluminosilicate suitable binder for producing ZCC with satisfactory outcomes is fly ash. [1]. The alkaline solution is often represented by the mixture of Sodium Hydroxide $NaOH$ (SH) with Sodium Silicate Na_2SiO_3 (SS) or the conjunction of Potassium Silicate K_2SiO_3 (KS) with Potassium Hydroxide KOH (KH) [8], [9]. The binder material such as fly ash (FA) is combined with an activating agent that offers the needed alkalinity to release the Si and Al. The mixture of aluminosilicate and alkaline activator is commonly called precursor.

Limited studies are available on the development and application of ZCC. The number of published articles on ZCC over are narrow the years, for example, SCOPUS databases showed limited published documents on ZCC between 1951 to reaching their maximum in 2021 with a slow growth rate over 20 years [10]. Hence, the nation nowadays needs an alternative material for the replacement of cement and this can be achieved by using natural resources or by-products in place of cement in the construction industry [11]. Although ferrocement normal and geopolymer concrete panels have been experimented with over the last years [12]–[17], very few researchers have conducted an examination on the performance of zero cement concrete slabs under monotonic loading with limited dimensions. Sakkarai et al (2021) [14] conducted a study on geopolymer mortar made, which represented by six heat-cured flat and folded panels (100×400×30) mm^3 subjected to monotonic loadings. They used the FA as the main precursor with an alkaline activator solution comprised of SS and SH. The results demonstrated that the impact strength of geopolymer folded panels surpassed that of geopolymer flat panels, with the energy absorbed at failure being directly proportional to the volume of reinforcement in the panels.

This research is limited to the laboratory investigation, environment, and conditions, which are consistent throughout the laboratory operation. Besides, industrial by-products' quality and specifications of the utilized FA might differ in terms of compositions, sources, and countries. Therefore, similar data gathered from other sources may be used in the next studies. If a different fraction is used for the analysis, this assumption might have an impact on the findings of this study. Also, due to different standard designs, critical values may vary.

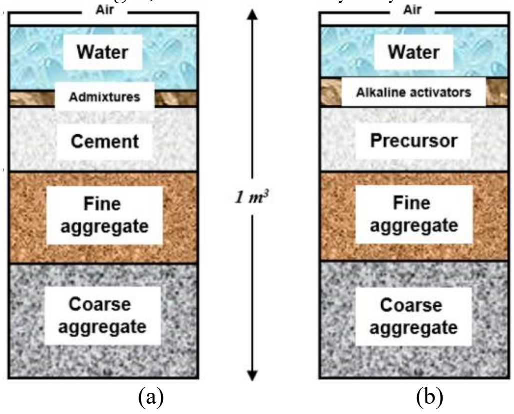

Figure (1): Main components [18] of (a) Normal and (b) Zero cement concrete

2. Research Significance

limited research and literature on zero-carbon concrete to obtain its superior strength, durability, enhanced sustainability, and greater energy savings for construction applications. However, considerable research still needs to be carried out to achieve zero carbon emissions or similar other concrete technology [10]. The integration between ZCC slabs and Applied loadings is still under the purview of many researchers, and thus, efforts have to be made in the direction of ambient curing and different blending of such as FA, GGBFS, silica fume, etc. to investigate further information about ZCCs. Thus, the current study aims to investigate the effect of monotonic loadings on the behavior of reinforced ZCC slabs according to various parametric studies: Slab thickness, bar spacing, and molarity concentrations.

3. Materials

Iraqi Ordinary Portland Cement was used to produce the normal concrete (NC) mixtures. Low calcium fly ash class F, according to ASTM C618 (2017) [19] classification, was used in this study. The fine aggregate used in the current research was natural sand passing from a 4.75mm sieve size. Coarse aggregate passing from 20 mm sieve size was locally obtained. The combination of two alkaline activators was used herein, namely Sodium Hydroxide $NaOH$ (SH) and Sodium Silicate Na_2SiO_3 (SS). The SH was obtained in the solid pellet state while the SS was in liquid state. 180-GS modified ViscoCrete was used as a superplasticizing chemical admixture that conforms to the ASTM C494 and BS-EN 934-2 [20], [21].

4. Mixture Design

Four batches were considered comprising normal concrete and ZCC. Table 1 shows the production of 1 m3 of normal and zero cement concrete quantities. Many trail mixtures were produced to reach the required optimal mix design by using a 180-litter size mixer, plastic cylinders and cubes, a digital scale, an air motor pump, and a vibrating table (Fig. 2). Before starting the mixing procedure, the mixer was maintained dry, clean, and free of water. This mixer was utilized for both NC and ZCC mixtures. The mixing program and mixing protocol are shown in Fig 3 and Fig. 4, respectively.

Table (1): Mixture proportion (kg/m^3)

Concrete type	w/c or ASS/FA	Water	Cement	FA	Coarse aggregate	Fine aggregate	Molarity (M)	SS/SH	SS	SH	SP (%)**
NCC	0.44	185	420	-	1054	697	-	-	-	-	1
ZCC-10M*	0.44	65	-	420	1054	640	10	2.5	132	53	1
ZCC-6M	0.44	65	-	420	1054	640	6	2.5	132	53	1
ZCC-14M	0.44	65	-	420	1054	640	14	2.5	132	53	1

* M=Molarity
** As a percentage of cementitious material

Figure (2): Instrumentations and tools for mixture design preparation

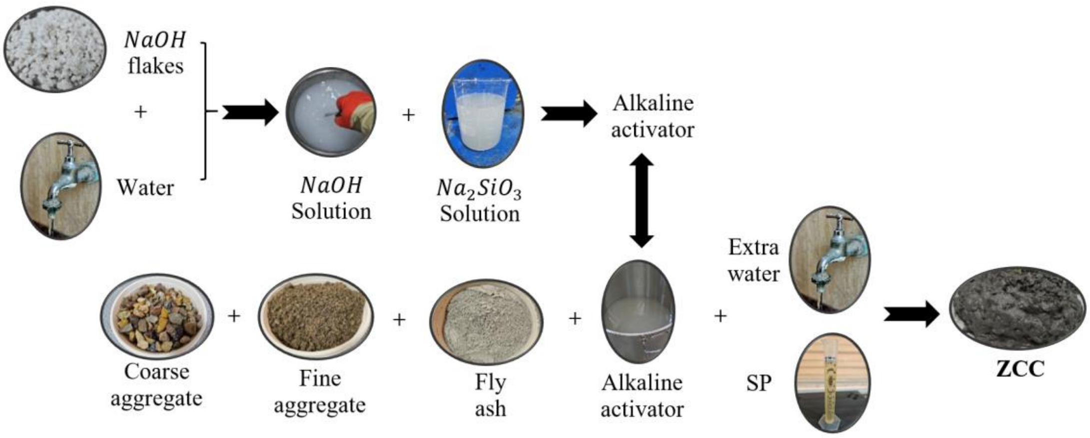

Figure (3): Mixing scheme of ZCC

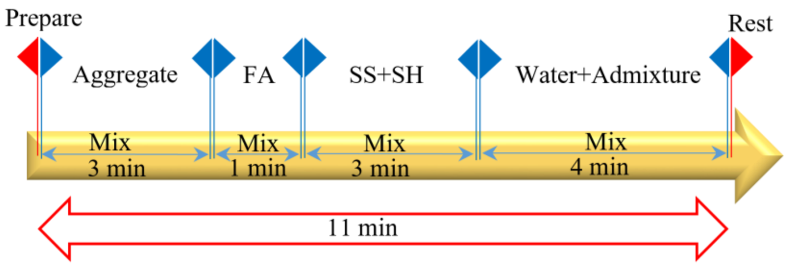

Figure (4): Mixing protocol

5. Slab geometric

Fig. 5 shows the geometrical and reinforcement details of tested RC slabs. The slabs were designed based on [22] specifications with dimensions of 1000mm×1000mm×80mm. A 20 mm clear concrete cover was used according to ACI 318M (2019) Table 20.5.1.3.1 [22]. To control cracking and resist moment at slab corners, steel reinforcement was designed according to ACI-318M (2019) [22] section 8.7.3. All the slabs have the dimensions of 1000 mm×1000mm×80 mm (except the group of varied thickness of 60 mm and 100 mm) with ϕ8 deformed bar reinforcement (8 mm diameter) with 150 mm spacing (except the group of varied spacing of 75 mm and 225 mm). Several parametric studies were used in this experimental work comprising thickness, bar spacing, and molarity. The tests and experiments were conducted at the laboratory of Al-Nahrain University/Civil Engineering Department.

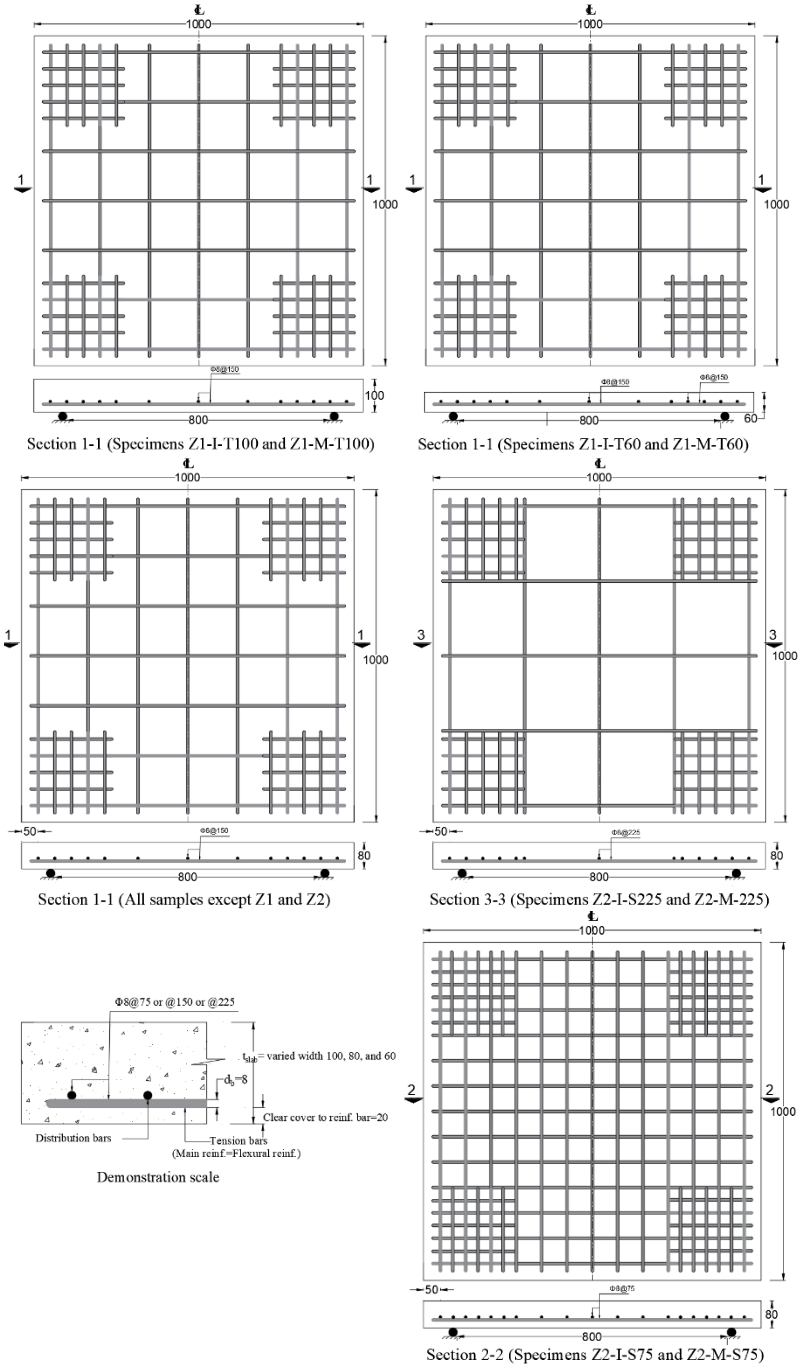

Figure (5): Geometrical and reinforcement description of the experimental slabs (All dimensions in mm)

6. Test Set-up

Eight RC slabs (including seven ZCC and one NC slab) were cast (Fig. 6)m ambient cured, and tested under a monotonic loading program (Fig. 7). The load was defined as a deflection increment by the universal hydraulic machine (Fig.). The loads were increased incrementally by about 10 kN/min up to failure. It is worth mentioning that the loadings were maintained several times to record loads, take photos, and observe crack responses.

Figure (6): Concrete casting

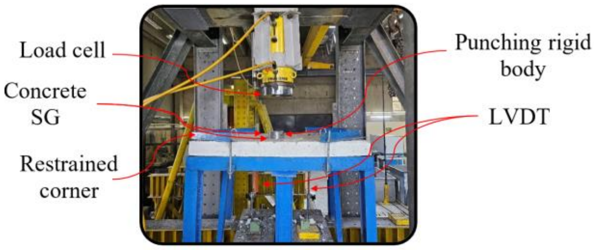

Figure (7): Test Scheme

7. Results and discussions:

The current section presents the slab responses in terms of load-deflection ($P-\delta$) relationship, load-strains ($P-\varepsilon$) relationship, load capacity, failure modes, and cracking patterns, under different levels of monotonic loads.

7.1 Load-deflection relationship

Fig. 8 shows the load-deflection ($P-\delta$) responses for each slab compared with the references slabs. For all slabs, the initial cracks were performed in accordance with the applied load levels relevant to the stiffness of each slab. It can be also seen that the cracks starting were apparently delayed for slabs in group 1 and group 2 relative to T60 and S225 respectively. The number of cracks was increased in companion with increasing loads and accordingly increasing the deflection up to the failure.

Fig. 8 demonstrates that increasing slab thickness from 60 mm to 80 mm and 100 mm enhances the slab stiffness. The 33.33% and 66.67% increase in thickness corresponded to reductions in mid-span deflection of approximately -6.45% and -51.99%, respectively. Additionally, the load capacity was increased by 27.12% and 87.63%, respectively. The slab with maximum thickness (100mm), represented by Z1-M-T100, exhibited the lowest deflection and highest load capacity, indicating its superior stiffness compared to Z1-M-T60 and Z1-M-T80 slabs. Thinner slabs were more prone to ductile failure, with increased deflection under lower loads. Decreasing bar spacing by 33.33% and 66.67% relative to 225 mm reduced deflection by about -12.11% and -36.29%, respectively, while improving load capacity by about 15.39% and 51.45%, respectively. Minimal changes in deflection and load were observed with varying molarity concentrations.

NI DIAdem software program was employed to determine the area under the $(P-\delta)$ curve, which represents the energy absorption (EA) capacity of the slab until failure. Fig. 9 shows various EA of the experimented RC slabs. It is obvious that the EA increased by about 14.33% and 47.76% when the slab thickness increased by 33.33% and 66.67%, respectively relative to 60mm thickness. Similarly, the escalation in EA capacity is about 8.67% and 33.31% due to a decrease in the bar spacing by 100% and 200%, respectively when compared to 225mm. On the other hand, slight change in EA when using various molarity concentrations in producing ZZC slabs.

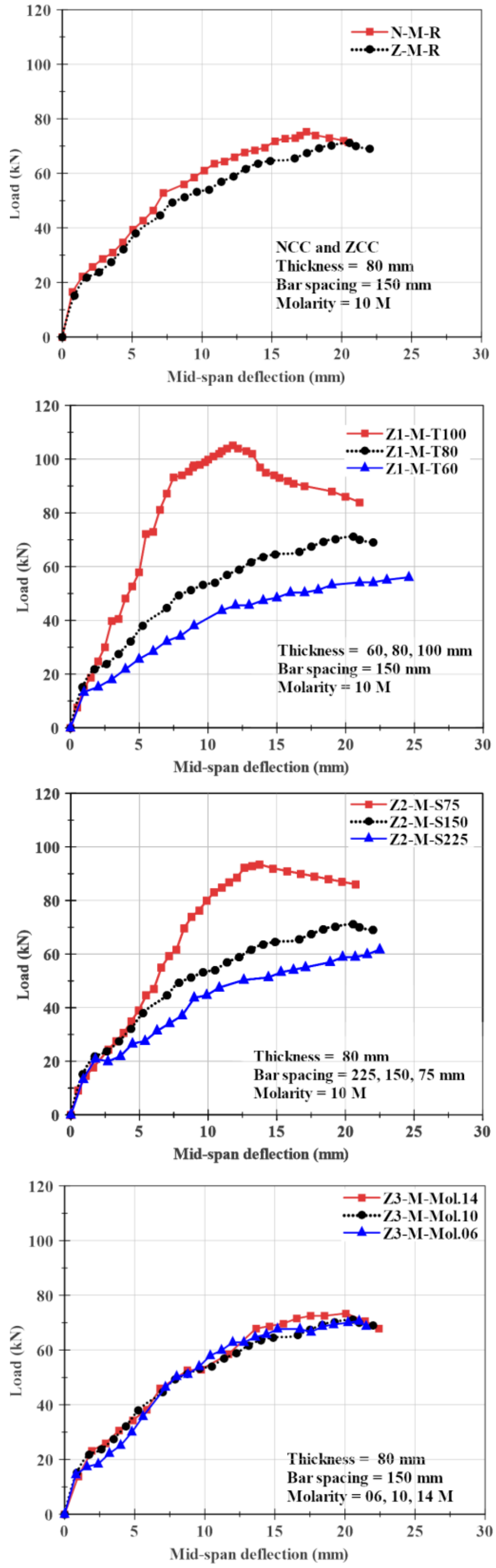

Figure (8): Load- central deflection

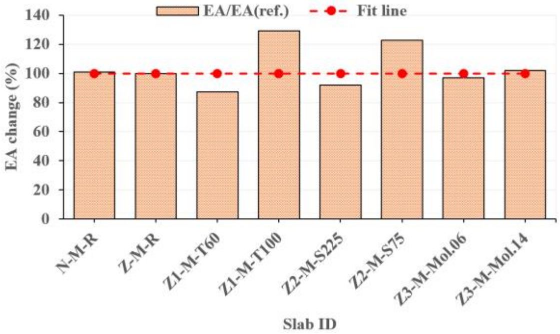

Figure (9): Increasing and decreasing in EA of ZZC slabs under monotonic loadings

7.2 Crack pattern and Failure mode

Investigation of the damage region and particularly the localized failure is usually more obvious from the general behavior of the member-deflected profile. Generally, most of the slab samples exhibited almost the same overall crack behavior (Fig. 10), however there were differences in the loading's intensity. There were not any cracks when the slab was initially loaded. The first cracks on the tension face of the slab developed around the loading region as the load progressed. Additional cracks start in the slab's center and spread to the slab edges as the load is increased to eventually fail by typically visible punching cone

It was observed that the number of cracks escalated but not enlarged/widened. Lastly, failure modes of punching shear were recorded in addition to the yielding of the flexural steel bars. A few flexural cracks on the slab compression face (top face) were noticed except at the circular loading rigid body zone which caused a localized penetration inside the midpoint slab center (Fig. 11). It was noticed that the number of cracks was higher in slab Z1-I-T60 and Z2-I-S225 than in other RC slab samples because cracks became less common as slab thickness and reinforcement rose, respectively.

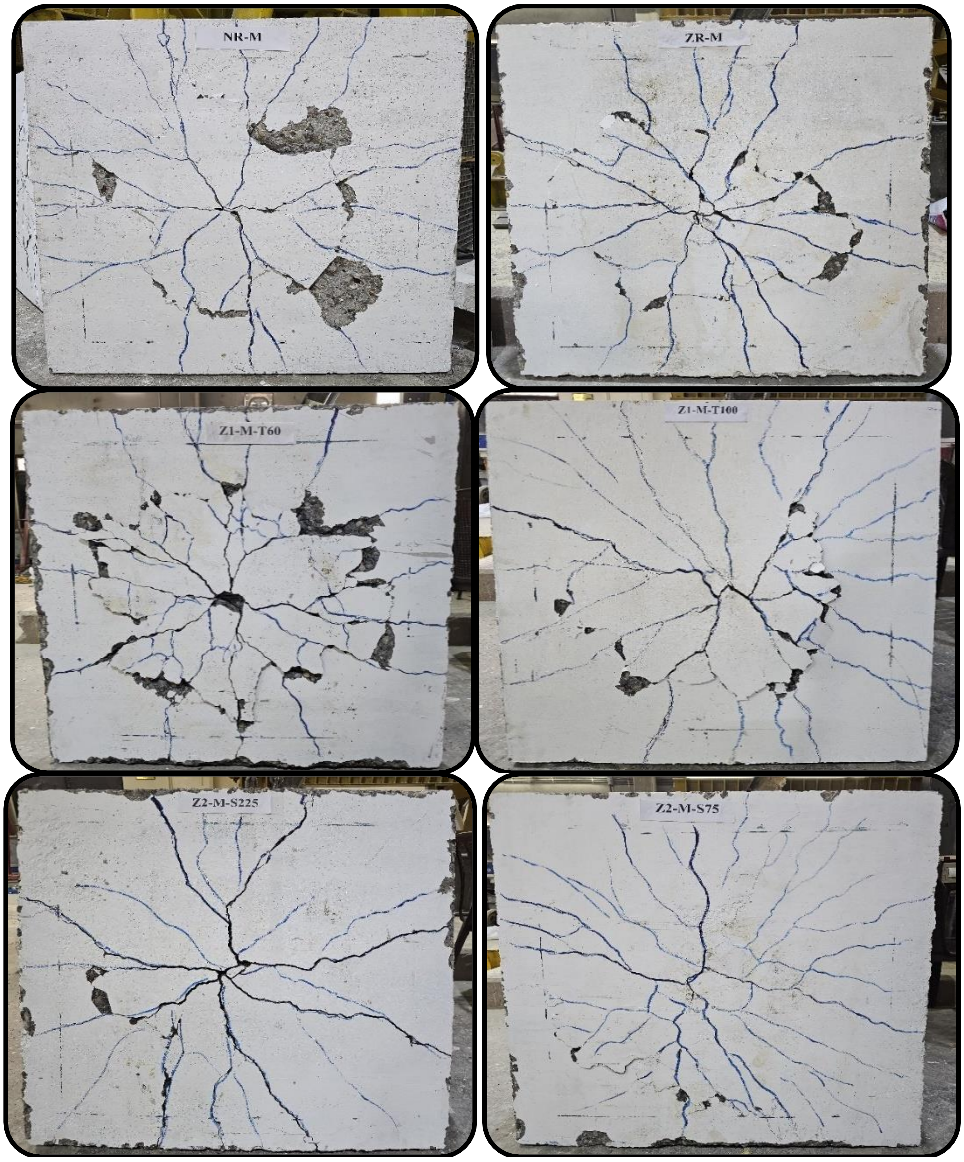

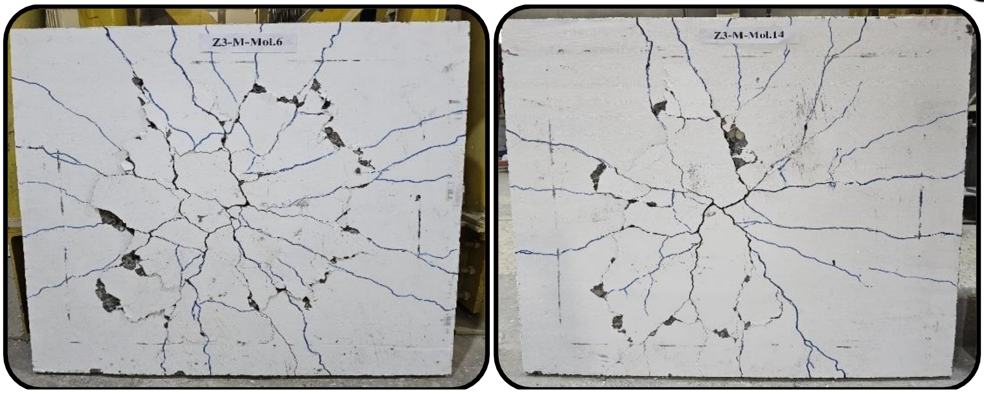

Figure (10): Crack pattern

Figure (11): Load- central deflection

8. Conclusion and Future Research Need

The objective of this research is to investigate the impact of various variables (i.e. slab thickness, bar spacing, and molarity concentration) on the performance of reinforced zero cement concrete slabs under monotonic loadings. The following findings can be concluded:

- Using free cement concrete is an optimal alternative to normal/conventional cement concrete (NCC) in terms of carbon emission, energy saving, and consuming waste material.
- The overall behavior of the reinforced ZCC slabs is similar to or slightly lower than the NCC under monotonic loadings.
- Increasing the thickness by about 33.33% and 66.67% relative to 60 mm thickness corresponded to reductions in mid-span deflection of approximately -6.45% and -51.99%, respectively. Moreover, the load capacity was increased by 27.12% and 87.63%, respectively.
- Decreasing bar spacing by 33.33% and 66.67% relative to 225 mm reduced deflection by about -12.11% and -36.29%, respectively, while improving load capacity by about 15.39% and 51.45%, respectively
- The energy absorption (EA) increased significantly when the slab thickness increased by 33.33% and 66.67%, respectively relative to 60mm thickness and when the bar spacing decreased by 100% and 200%, respectively compared to 225mm. On the other hand, slight change in EA when using various molarity concentrations in producing ZZC slabs.
- Most of the slab samples exhibited almost the same overall crack behavior, in spite of there being differences in the loadings intensity.

One of the constraints of this study is the lack of standards or code of practice for ZCCs related to their mixture design, mixing procedure, mechanical properties formulas, etc., and hence, more efforts must be conducted to standardize codes and reports. Besides, Other dynamic and static structural experiments have to be made to investigate the performance of ZCC structural members.

9. References:

[1] V. S. Athira, V. Charitha, G. Athira, and A. Bahurudeen, "Agro-waste ash based alkali-activated binder: Cleaner production of zero cement concrete for construction," *J. Clean. Prod.*, vol. 286, p. 125429, 2021, doi: 10.1016/j.jclepro.2020.125429.

[2] J. Davidovits, "High-Alkali Cements for 21st Century Concretes," *ACI Symp. Publ.*, vol. 144, no. Special Publication, pp. 383–398, 1994, doi: 10.14359/4523.

[3] V. Masson-Delmotte *et al.*, "Global warming of 1.5 C," *An IPCC Spec. Rep. impacts Glob. Warm.*, vol. 1, no. 5, p. 36, 2018, [Online]. Available: https://www.ipcc.ch/sr15/

[4] T. Bakharev, J. G. Sanjayan, and Y.-B. Cheng, "Sulfate attack on alkali-activated slag concrete," *Cem. Concr. Res.*, vol. 32, no. 2, pp. 211–216, 2002, doi: https://doi.org/10.1016/S0008-8846(01)00659-7.

[5] E. Gomaa, S. Sargon, C. Kashosi, and M. ElGawady, "Characterization and Performance of Zero-Cement Concrete," United States, Missouri, 2018. [Online]. Available: https://rosap.ntl.bts.gov/view/dot/37913

[6] R. J. Thomas and S. Peethamparan, "Alkali-activated concrete: Engineering properties and stress–strain behavior," *Constr. Build. Mater.*, vol. 93, pp. 49–56, 2015, doi: https://doi.org/10.1016/j.conbuildmat.2015.04.039.

[7] A. Bisarya, R. K. Chouhan, M. Mudgal, and S. S. Amritphale, "Fly ash based geopolymer concrete a new technology towards the greener environment: A review," *Int. J. Innov. Res. Sci. Eng. Technol*, vol. 4, no. 12, pp. 12178–12186, 2015, doi: 10.15680/IJIRSET.2015.0412089.

[8] M. I. A. Aleem and P. D. Arumairaj, “Optimum mix for the geopolymer concrete,” *Indian J. Sci. Technol.*, vol. 5, no. 3, pp. 2299–2301, 2012, doi: 10.17485/ijst/2012/v5i3.8.
[9] M. I. A. Aleem and P. D. Arumairaj, “Geopolymer concrete–a review,” *Int. J. Eng. Sci. Emerg. Technol.*, vol. 1, no. 2, pp. 118–122, 2012, doi: 10.7323/ijeset/v1_i2_14.
[10] M. Wasim, A. Abadel, B. H. Abu Bakar, and I. M. H. Alshaikh, “Future directions for the application of zero carbon concrete in civil engineering – A review,” *Case Stud. Constr. Mater.*, vol. 17, p. e01318, 2022, doi: 10.1016/j.cscm.2022.e01318.
[11] V. K. J. Bohra, R. Nerella, and S. R. C. Madduru, “Material properties, processing & characterization of fly ash based geopolymer,” *Mater. Today Proc.*, vol. 19, pp. 2617–2621, 2019, doi: 10.1016/j.matpr.2019.10.099.
[12] S. S. Arun Kumar, A. Madhavan, and S. Dharmar, “Experimental Srudy on Impact Resistance of Geopolymer Ferrocement Flat Panel,” *SSRG Int. J. Civ. Eng.*, no. Special Issue ICRTCETM-Part 4, pp. 278–282, 2017, [Online]. Available: https://www.internationaljournalssrg.org/special_issues/specialissues_paperlist/5-Part4-8
[13] M. Rajendran and N. Soundarapandian, “An experimental investigation on the flexural behavior of geopolymer ferrocement slabs,” *J. Eng. Technol.*, vol. 3, p. 97, Aug. 2013, [Online]. Available: https://link.gale.com/apps/doc/A349640871/AONE?u=anon~1a1532df&sid=googleScholar&xid=7e50d4e6
[14] D. Sakkarai and N. Soundarapandian, “Strength Behavior of Flat and Folded Fly Ash-Based Geopolymer Ferrocement Panels under Flexure and Impact,” *Adv. Civ. Eng.*, vol. 2021, p. 2311518, 2021, doi: 10.1155/2021/2311518.
[15] S. S. Hiremath, “FLEXURAL BEHAVIOUR OF GEOPOLYMER BASED FERROCEMENT PANELS,” *Int. J. Appl. Eng. Res.*, vol. 13, no. 7, pp. 284–291, 2018.
[16] M. Ramalingam, P. Mohan, P. Kathirvel, and G. Murali, “Flexural Performance and Microstructural Studies of Trough-Shaped Geopolymer Ferrocement Panels,” *Materials*, vol. 15, no. 16. p. 5477;, 2022. doi: 10.3390/ma15165477.
[17] M. Rajendran and N. Soundarapandian, “Geopolymer ferrocement panels under flexural loading,” *J. Sci. Eng. Compos. Mater.*, vol. 22, no. 3, pp. 331–341, 2013, doi: 10.1515/secm-2013-0012.
[18] N. Li, C. Shi, Z. Zhang, H. Wang, and Y. Liu, “A review on mixture design methods for geopolymer concrete,” *Compos. Part B Eng.*, vol. 178, p. 107490, 2019, doi: https://doi.org/10.1016/j.compositesb.2019.107490.
[19] ASTM-C618, “Standard specification for coal fly ash and raw or calcined natural pozzolan for use in concrete,” in *Annual Book of ASTM Standards*, West Conshohocken, PA, USA: ASTM American Society for Testing and Materials:, 2017, p. 5. doi: 10.1520/C0618-17.
[20] ASTM-C-494C/494M, “Standard Specification for Chemical Admixtures for Concrete,” in *Annual Book of ASTM Standards Volume: 04.02*, American Society for Testing and Materials, 2019, p. 10. doi: 10.1520/C0494_C0494M-17.
[21] BS-EN/934-2, “Admixtures for Concrete, Mortar and Grouting, Part 2: Concrete admixtures — Definitions, requirements, conformity, marking and labelling.” British Standard Institution, London, p. 28, 2001.
[22] ACI-318M, “Building Code Requirements for Structural Concrete,” in *American Concrete Institute Standards*, Southern California: American Concrete Institute, 2019.